

MODIFIED WEB SLENDERNESS CLASSIFICATION FOR COMPOSITE GIRDERS IN CODE PROVISIONS.

Ahmed Mohamed Abdelrahman¹, *Manar Maher Hussein² and Walid Abdel-Latif Attia³

^{1,2,3}Faculty of Engineering, Cairo University, Egypt

*Corresponding Author, Received: 30 Dec. 2020, Revised: 25 Jan. 2021, Accepted: 06 Feb. 2021

ABSTRACT: Composite girder is one of the main structural systems used in bridges and buildings. The same slenderness limits requirements for steel sections are used also for the composite sections in most specifications without considering the effect of concrete slabs. In fact, for composite sections under positive moments, the compression concrete slab restrains the buckling of the top flange and the compressed part of the web, in addition the steel plates behave plastically up to failure. By accounting concrete slabs attached to the steel compression elements, the section may be placed in more favorable class. The main objective of this study is to verify a reasonable relaxed slenderness limits for steel compact composite sections compared to compact steel section only and investigate the influences of the span length of girder and the concrete strength of slab, on the slenderness limits. An extensive parametric study using ANSYS, a commercial finite element (FE) software, was held using different web slenderness, various concrete strengths and girder lengths. The section classifications were evaluated, and the results were compared to the Egyptian code, Eurocode and AASHTO. A new relaxed equation and new classification limits have been developed considering the effect of the concrete slab strength.

Keywords: Composite girders; Web slenderness; Ultimate flexural strength; Egyptian Code; ANSYS

1. INTRODUCTION

Considering its influence on reduction in cost and time, composite steel-concrete girders, especially for medium to large bridges' spans and multi-story steel wide frames, have achieved high market share. Composite girders are horizontal structures, in most cases, consisting from steel and concrete. For simple composite girders, the steel section is located in tension region and the concrete slab located in the compression region. These two materials connected by metallic devices called shear connectors. Gupta [1] stated that most available codes' formulas are based on linear experimental techniques not accounting the material or geometric nonlinearities and not considering the effect of the concrete slab in composite sections. Taleb and Ammari [2] indicated that the theoretical simplicity of supports is fulfilled by certain dimensions of flanges. The concrete slab fixation at the composite section eliminates the web local buckling length at least in loading direction. An in-plane deformation happens axially before transverse buckling and shear deformation as concluded by Musa [3]. Thus, concrete slab also provides practically more in plane resistance for the axial deformation compared to the steel section only. Liu [4] explained that some of the empirical methods could be more applicable and non-conservative in accounting the flexural

capacity of simply supported composite beams considering various degrees of shear connection. For full integration composite compact section with high yield strength steel section, the failure can occur due to concrete crushing or steel plastic failure [5]. However, for compact sections with higher steel yield strengths, crushing of the concrete slab may take place before reaching section full plastic moment capacity. All the girders were designed using current codes such as AASHTO [6] and EUROCODE [7] to predict the flexural strength of sections with D_p/D_t in the linear range (Figs.1-2), where D_p is the position of the plastic neutral axis and D_t is the total depth of section. A proposed equation was expressed as a function of D_p/D_t ratio[5]. Duc and Okui [8]and [9], studied the influence of using composite high strength steel with ultimate strength equals to 500 N/mm² and 700 N/mm² on the web slenderness limits. They concluded that using high strength steel to both homogeneous and hybrid sections increase significantly the web slenderness limits. The behavior of composite girders under combined negative moment and shear and with web local buckling effects was investigated in [10]and [11].

In this study, the concrete strength was considered as a factor to produce new equation and classifications limits. The research objectives were to achieve a good understanding for the types of predominate failure modes of Steel-Concrete composite girders and provide a less strenghen

design tendency. This was implemented by verifying a reasonable slenderness limits for steel compact composite sections relaxed compared to those for compact steel section only and accounting for the material plasticity behavior, buckling and concrete crushing. Also, by investigating the effects of girder span length and slab concrete strength on the slenderness limits and applying these studies to the Egyptian code of practice for steel construction [12]. Two yield steel strengths (240 and 360N/mm²) were applied in [13]. The present study was limited to high yield steel strength of 360N/mm², not extended to study connection failure or slipping of shear connectors, full interaction composite. In addition, this study is limited to shored composite girders and not extended to the influence to the effect of the initial moment or residual stresses effect.

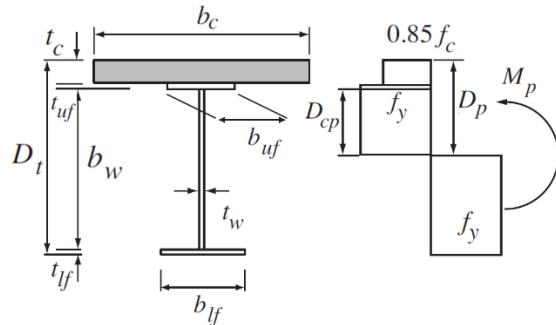


Fig. 1 Stress distribution in compact section [14]

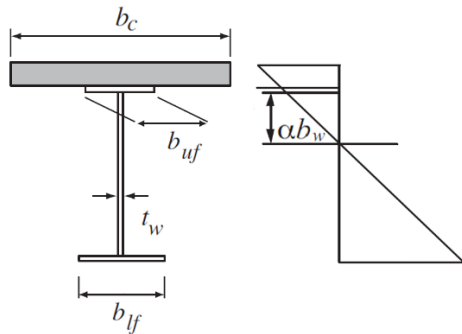


Fig. 2 Theoretical strain in compact section [14]

2. METHODOLOGY AND VALIDATION

In order to accomplish the study, finite element analysis using a commercial finite element software ANSYS. This software is able to simulate the overall non-linear plastic behavior of simply supported composite beams including buckling of the steel elements and cracking of the concrete slab.

2.1 Codes Classifications

Specifications [12] and [6] classified steel sections according to buckling behaviours to three types, compact, non-compact and slender as shown

in Fig.3. While according to [7], the composite sections are classified into four categories (Table 1), allowing using plastic design method only for Class 1 and 2 sections, while [12] and [6] allow it for the compact section only. Section classifications are shown in Table1, with parameters as defined in the relevant codes and Figs. 1-3; M_y , M_p and M_{max} are yield, plastic and ultimate moments respectively. While b_w , t_w , ε and Ψ are web height, web thickness, maximum strain and ratio between upper to lower flanges stresses respectively. While D_{cp} is the depth of web in compression and α is the ratio between the location of axis of bending to the web height. In fact, most available codes' formulas are based on linear experimental techniques, not accounting the material or geometric nonlinearities and not considering for the effect of concrete slab in composite sections [1].

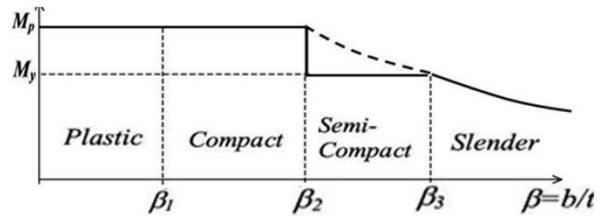


Fig. 3 Moment capacities of sections [15]

2.2 Structural Buckling and plastic behavior

Buckling is one of the most critical failure modes in steel structures under compression or bending loads [16]. The main types of local buckling behaviors of the steel elements were shown in Fig. 4 [17]. These sections can be regarded as a combination of individual plate elements connected together to form the required shape. Different types of overall structural buckling were presented in Fig. 5 [18]. All codes and standards consider the buckling as one of the main governing factors to account the strength of the steel structural elements although that the total collapse not necessarily developed by buckling of an edge-supported thin plates and the plates can generally support more loads greater than critical local buckling loads load.

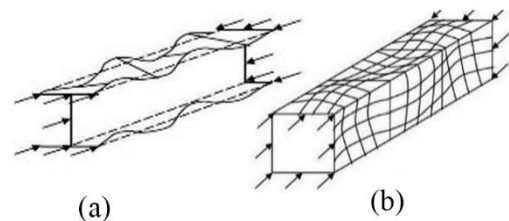


Fig. 4 Local buckling a) open b) closed section.

Table 1: Section Classifications AASHTO [6], EUROCODE [7] and ECP-LRFD [19]

| Design Code | Section Class | Definitions | Web Slenderness Limits |
|--------------------|---------------|--|--|
| AASHTO (2005) | Compact | $M_{max} > M_p$ | $2D_{cp}/t_w \leq 3.76 \sqrt{E_s/F_y}$ |
| | Non-Compact | $M_p > M_{max} \geq M_y$ | $2D_{cp}/t_w \leq 5.7 \sqrt{E_s/F_y}$ |
| | Slender | $M_{max} < M_y$ | Other than those Above |
| EUROCODE (2001) | Class 1 | $M_{max} \geq M_p$ Sufficient Rotational Capacity | $b_w/t_w \leq \begin{cases} 36\epsilon/\alpha & \text{for } \alpha \leq 0.5 \\ 396\epsilon/(13\alpha - 1) & \text{for } \alpha > 0.5 \end{cases}$ |
| | Class 2 | $M_{max} \geq M_p$ Limited Rotational Capacity | $b_w/t_w \leq \begin{cases} 41.5\epsilon/\alpha & \text{for } \alpha \leq 0.5 \\ 456\epsilon/(13\alpha - 1) & \text{for } \alpha > 0.5 \end{cases}$ |
| | Class 3 | $M_{max} \geq M_y$ | $b_w/t_w \leq \begin{cases} 42\epsilon/(0.67 + 0.33\psi) & \text{for } \psi < -1.0 \\ 62\epsilon/(1 - \psi)\sqrt{-\psi} & \text{for } \psi \geq -1.0 \end{cases}$ |
| | Class 4 | $M_{max} < M_y$ | Other than those Above |
| ECP-LRFD (2012) | Compact | $M_{max} > M_p$ | $b_w/t_w \leq \begin{cases} 699/\sqrt{F_y}/(13\alpha - 1) & \text{for } \alpha \leq 0.5 \\ (36.6/\alpha)/\sqrt{F_y} & \text{for } \alpha > 0.5 \end{cases}$ |
| | Non-Compact | $M_p > M_{max} \geq M_y$ | $b_w/t_w \leq \begin{cases} 111/(1 - \psi)\sqrt{-\psi}/\sqrt{F_y} & \text{for } \psi \leq -1.0 \\ 222/\sqrt{F_y}/(2 + \psi) & \text{for } \psi > -1.0 \end{cases}$ |
| | Slender | $M_{max} < M_y$ | Other than those Above |

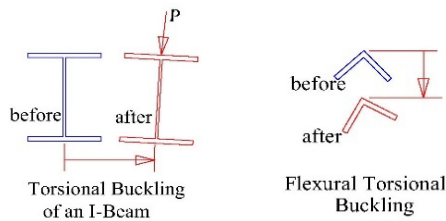


Fig.5 Types of overall buckling

For plate girders consisting from three plates, considering (b) as plate length and (t) as plate thickness and $\beta=b/t$. Sections of steel structures can be classified according to plastic behavior (Fig. 3):

- Plastic sections, when section can reach its full-plastic moment M_p and allow rotation at or after the plastic moment.
- Compact cross-sections, when section can reach its full-plastic moment M_p but the rotation could not be developed.
- Non-Compact cross-sections, when local buckling prevents the section from reaching its full-plastic moment M_p .

- Slender cross-sections when the local buckling prevent ultimately the reaching of the yield.

Web slenderness is one of the most important influence on flexural strength of composite girder.

2.3 Numerical Study

For Steel Plates, ANSYS Three-dimensional four-node shell element, SHELL43 were used with three translations in x, y and z in each node to achieve the compatibility condition with translation in x, y and z in adjacent brick element to it. An eight-node solid element, Solid65, was used to model the concrete with three degrees of freedom at each node—translations in the nodal x, y, and z directions. The element is capable of plastic deformation, cracking in three orthogonal directions, and crushing. Mesh dimensions of both elements types for the section equals to 50mm in both directions. Figure 6 shows the overall FE model. Constraining the steel girder and concrete slab at the connected joints in the three transitions directions simulated the full integrated simply supported girder composite action. The

static loading applied was chosen to be in the shape of point loads which were applied by means of displacement control method, the loads were increased incrementally. Vertical displacements were applied at five adjacent bottom joints in the middle section' lower flange of the span to distribute the effect of loading (Fig. 7-a). The strain values were considered by adding the Von mises elastic strains to the equivalent plastic strains produced by ANSYS finite elements results. Figure 7-b shows the boundary conditions of supports; one end of the girder was restrained against transitional movements in the three orthogonal directions X, Y and Z, while the other was restrained in Y and Z directions. The restraints were performed nearly at the center of gravity of the steel structure section.

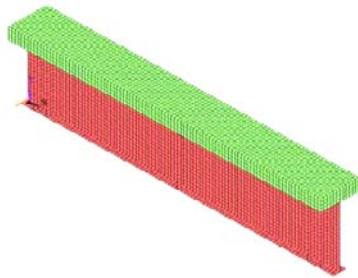


Fig. 6 Overall FE model for the composite section

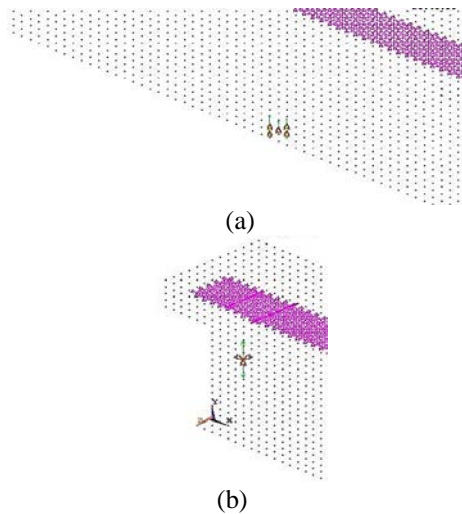


Fig. 7 Boundary Conditions a) Loading nodes in numerical model, b) Support boundary conditions.

2.4 Validation of the Model

The reliability of the FE model of composite beams is validated by comparison with experimental study. The reference specimen [20] was tested experimentally and analytically using DIANA, a finite element software program. Figure 8 shows the girder specimens with a span length of 9.00 m loaded in the middle of the specimen. I shaped steel girders were designed with SM400A grade steel (Yield strength 300 MPa, Ultimate

strength 450 MPa and 28% elongation) while the concrete strength of the slab is 45 MPa. A 9.00m span girder was used as a reference to validate the present ANSYS F.E. method in this study. Fig. 9 shows a comparison of the Load – displacement curves of the Okui's [20] experimental results and the ANSYS verification model; the figure showed a good agreement in the results of the two specimens (less than 5% difference).

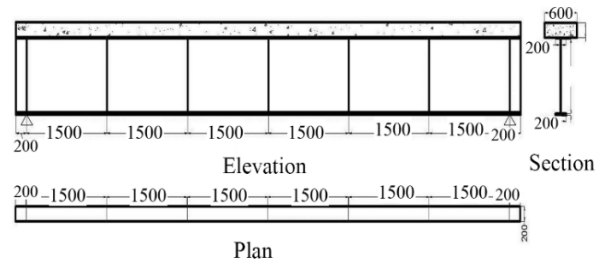


Fig. 8 Reference Specimen [20]

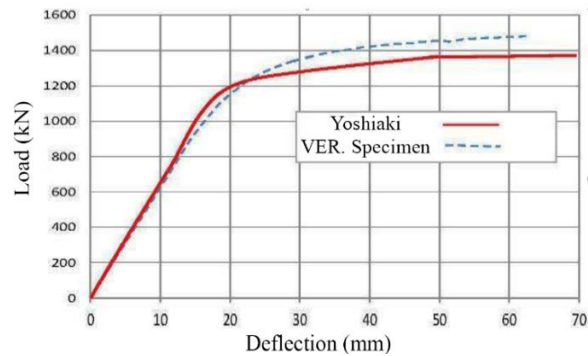


Fig. 9 Compared Load-Deflection relationship

3. PARAMETRIC STUDY

Table 2 shows the properties of the specimens used in this study. The two groups depending on the concrete strengths, 20 N/mm² and 40 N/mm², (0.2 and 0.4 t/cm²), were divided to three types referenced to the used steel web width/thickness plate original slender classification: 13, 23 and 33. At this study, F_{yw} and F_{yf} are yield strength of the specimen's web and flanges respectively, were equal both to 360N/mm². The original section classification according to ECP-LRFD [12] steel structure classification was shown also. All specimens' lower flanges were 30mm thickness and the upper flanges with 5mm thickness. Specimens were chosen to fulfill that the linear plastic neutral axis is located on the steel upper web. Span length shortest specimen's length, 4.5 m, A-specimens, represented average of the maximum length limiting laterally unbraced length for inelastic lateral torsion buckling of steel structural girders, L_r as per [12]. Other spans, 9.00m, B-specimens, and 18.00m, C-specimens, were duplicated of the shortest length. Concrete slab width, 600 mm, equivalent to three times the upper flange width

($B_f=200\text{mm}$) and one eighth of the shorter span
Table 2- Specimens Properties

length, while the depth was 200mm.

| | | L | Web | b_w | t_w | b_w/t_w | Status |
|---------------------------|-------|-------|---------|-------|-------|-----------|-------------|
| | | m | mm | mm | mm | | ECP LRFD |
| Conc. Strength 0.20 Spec. | 20A13 | 4.50 | 1000X20 | 1000 | 20 | 50 | C |
| | 20A23 | 4.50 | 1000X10 | 1000 | 10 | 100 | NC |
| | 20A33 | 4.50 | 1000X5 | 1000 | 5 | 200 | S |
| | 20B13 | 9.00 | 1000X20 | 1000 | 20 | 50 | C |
| | 20B23 | 9.00 | 1000X10 | 1000 | 10 | 100 | NC |
| | 20B33 | 9.00 | 1000X5 | 1000 | 5 | 200 | S |
| | 20C13 | 18.00 | 1000X20 | 1000 | 20 | 50 | C |
| | 20C23 | 18.00 | 1000X10 | 1000 | 10 | 100 | NC |
| | 20C33 | 18.00 | 1000X5 | 1000 | 5 | 200 | S |
| Conc. Strength 0.40 Spec. | 40A13 | 4.50 | 1000X20 | 1000 | 20 | 50 | C |
| | 40A23 | 4.50 | 1000X10 | 1000 | 10 | 100 | NC |
| | 40A33 | 4.50 | 1000X5 | 1000 | 5 | 200 | S |
| | 40B13 | 9.00 | 1000X20 | 1000 | 20 | 50 | C |
| | 40B23 | 9.00 | 1000X10 | 1000 | 10 | 100 | NC |
| | 40B33 | 9.00 | 1000X5 | 1000 | 5 | 200 | S |
| | 40C13 | 18.00 | 1000X20 | 1000 | 20 | 50 | C |
| | 40C23 | 18.00 | 1000X10 | 1000 | 10 | 100 | NC |
| | 40C33 | 18.00 | 1000X5 | 1000 | 5 | 200 | S |

4. RESULTS AND DISCUSSIONS

Table 3 summarizes the results of flexural moments for the specimens. Calculated plastic and yield moments in addition to flexural moments at failure for the F.E. specimens were shown. Yield and plastic moments were determined analytically for each section using the first principal's assumptions. M_u represented the minimum of ANSYS FE's steel ultimate moment at failure or the moment corresponding to plain concrete maximum allowable strain limit equaled to the second boundary limit, 0.0035, whichever less. Maximum moment at the first concrete cracking was considered as the local buckling beginning of the failure process propagation. This was due that after cracking moment, the section could not still act with its full restraint actions to out of plane effects for the upper flange and the part of web under compression. Then, the new status of the sections was based on comparing M_u to M_y and M_p . If M_u equaled or exceeded the value of the M_y , this was an indication for reaching the non-compact limit while if it reached M_p this was considered still within the compact limits. Otherwise, if the value of M_u was below M_y value, it was considered in the slender classification category.

For the medium span specimens 9.00m, B-specimens, it was observed that the initially

classified non-compact and even slender sections have been upgraded in performance to act as a compact section reaching its relevant plastic moment value regardless the web thickness. For originally classified compact sections of the shortest length, 4.50m, A-specimens, the ultimate moments were less than the plastic capacity moments. This could be referred to that for shorter specimens, the failure criteria governed could be predominated by the capacity of the shear strength of the section and shear buckling and would not allow enough rotation. the predominated failure is most cases related to shear failure not for moment. For longer spans of 18.0m, C-specimens, the compact sections remained compact for the two used types of concrete strengths, while for the non-compact section even if it allowed more rotations, but the ultimate moment, defined with respect to concrete crushing, did not reach the plastic moment for higher concrete strength. This could be also related to the influences of out of plane effects under the conditions of dimensions of the concrete slabs and steel sections used in this study. Fig.10 shows the relation between slenderness limits represented by web width/web thickness and the result value of α evaluated from the finite element analysis. Fig.11 shows the moment verses rotation relationships for C's specimen which indicated the higher level of ductility performance with respect to

the others specimens' lengths. It was observed from Fig. 10 that the three variable specimens with Table 3: Specimens Results

from Fig. 10 that the three variable specimens with

| | | Moments N.mm (x10E5) (ton.cm) | | | | | | ECP- Status | New Status |
|---------------------------------|-------|----------------------------------|----------------|----------------|--------------------------------|--------------------------------|--------------------------------|----------------|---------------|
| | | M _y | M _u | M _p | M _u /M _y | M _u /M _p | M _p /M _y | | |
| Concrete Strength 0.20 Spec. | 20A13 | 3129.4 | 3600.0 | 4325.5 | 1.15 | 0.83 | 1.38 | C | NC |
| | 20A23 | 2346.1 | 2961.5 | 3423.5 | 1.26 | 0.87 | 1.46 | NC | NC |
| | 20A33 | 1902.8 | 2005.0 | 2969.5 | 1.05 | 0.68 | 1.56 | S | NC |
| | 20B13 | 3129.4 | 5060.8 | 4325.5 | 1.62 | 1.17 | 1.38 | C | C |
| | 20B23 | 2346.1 | 3670.0 | 3423.5 | 1.56 | 1.07 | 1.46 | NC | C |
| | 20B33 | 1902.8 | 3201.6 | 2969.5 | 1.68 | 1.08 | 1.56 | S | C |
| | 20C13 | 3129.4 | 4535.0 | 4325.5 | 1.45 | 1.05 | 1.38 | C | C |
| | 20C23 | 2346.1 | 3545.3 | 3423.5 | 1.51 | 1.04 | 1.46 | NC | C |
| | 20C33 | 1902.8 | 2570.6 | 2969.5 | 1.11 | 0.71 | 1.56 | S | NC |
| Concrete Strength 0.40 Spec. | 40A13 | 3322.0 | 4423.1 | 5381.2 | 1.33 | 0.82 | 1.62 | C | NC |
| | 40A23 | 2442.5 | 3346.0 | 4300.7 | 1.37 | 0.78 | 1.76 | NC | NC |
| | 40A33 | 1945.8 | 2456.7 | 3850.5 | 0.86 | 0.44 | 1.98 | S | NC |
| | 40B13 | 3322.0 | 5626.0 | 5381.2 | 1.69 | 1.05 | 1.62 | C | C |
| | 40B23 | 2442.5 | 4456.0 | 4300.7 | 1.82 | 1.04 | 1.76 | NC | C |
| | 40B33 | 1945.8 | 4032.6 | 3850.5 | 2.07 | 1.05 | 1.98 | S | C |
| | 40C13 | 3322.0 | 5250.0 | 5381.2 | 1.76 | 1.09 | 1.62 | C | C |
| | 40C23 | 2442.5 | 3882.5 | 4300.7 | 1.18 | 0.67 | 1.76 | NC | NC |
| | 40C33 | 1945.8 | 2923.5 | 3850.5 | 1.14 | 0.58 | 1.98 | S | NC |

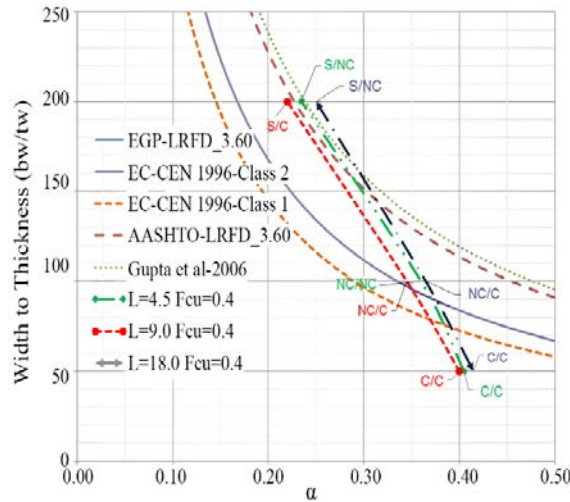


Fig. 10 Specimens results for α & b_w/t_w relation.

length 9.00m behaved as a compact section regardless their web thickness with lowest value of α , thus these specimens were considered the base points to evaluate the new relaxed equation as clarified above. The study led to a proposed derived equation Eq. (1) representing the boundary limit between Compact and Non-compact taking the steel and concrete strengths into consideration.

$$b_w/t_w \leq [350e^{-7.15\alpha}]^{\frac{5.40}{\sqrt{F_y}}} \sqrt{(0.2/F_{cu})} \quad (1)$$

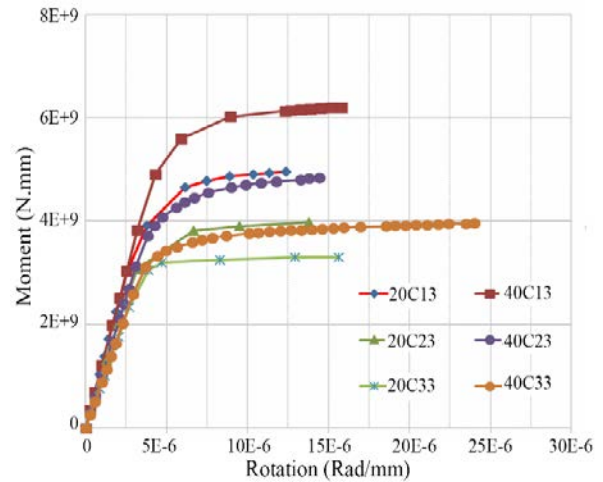


Fig. 11 Moment-Rotation for C's specimens

Where $\alpha = D_{cp}/b_w$, F_y yield strength of web in N/mm², F_{cu} yield strength of concrete in N/mm², b_w web maximum dimension (length) in mm, t_w web minimum dimension (thickness) in mm. Fig. 12 shows the proposed equation relative to the two concrete strength categories used in this study with respect to the variable codes mentioned compared with other codes' curves. It is clear that the using concrete slab dimensions and strength introduced new factors totally different to steel structural material. It is also observed that accounting

concrete slab provided a clear relaxation for the limit requirements between compact and non-compact sections: sections considered non-compact in the Egyptian Code of practice reached their compactness limit in the proposed equation. This will have a considerable reduction in the cost of composite girders construction.

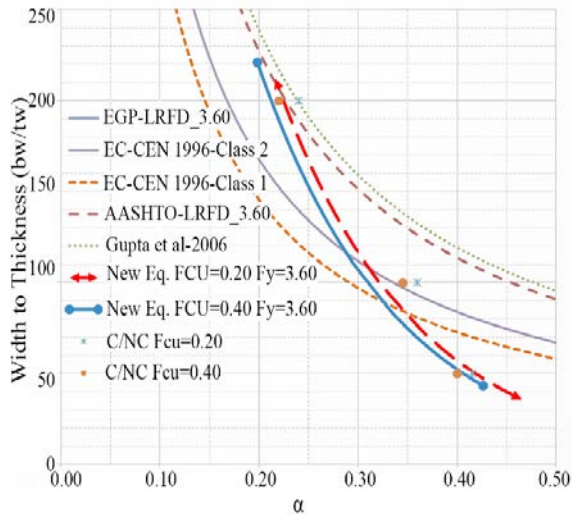


Fig. 12 Proposed Equation Curves

5. CONCLUSION

In this study, a series of numerical analyses were conducted using two types of concrete strengths with variable spans to study their effect on the slenderness limit. Based on the results obtained, a modified slenderness limits for composite girders are proposed. The research results are as follows:

1. ECP-LRFD is nearly similar to the Eurocode class 2 in the Compact - Non-compact limits. In addition, the ECP-LRFD is significantly conservative compared to the obtained results and also to AASHTO limits.
2. A new relaxed equation and new classifications limits have been developed considering the effect of the concrete slab strength. This contribution helped to improve the Egyptian code for a more accurate values and more economic sections.
3. Gupta curve is slightly relaxed than the AASHTO one at the compact- non compact limits as Gupta only considers one type of concrete strength with only one length span.
4. The increase in concrete strength has a negative influence on the slenderness limits, this is related to the reduction of the D_{cp}/D_p and to the crushing of concrete. This may lead that concrete with less compressive strength is more economic in the composite concrete-steel girders. Most codes provide a limit for ductility

to prevent concrete crushing, this limit have to be considered in the ECP-LRFD.

5. Knowing that the flexural ductility is better to be observed from the rotation verses bending moment curves, it was shown that the increase in regularity performance was directly proportional to the specimen's span length and the best specimens which show good global ductility performance were the longest spans.
6. Lengths for limiting lateral unbraced for full plastic bending capacity (L_p), for inelastic lateral torsional buckling (L_r) and for using plastic design (L_{pd}) have to be revised in the composite section in code, as the upper flange is already restricted from moving and its strength has no effect on the compression behavior of the section. ECP-LRFD maximum lengths relative to beginning the local buckling for the steel structure sections is not applicable for composite sections.
7. This research has offered a good preliminary approach, but further study is still required on the implication of its recommendations, to enlarge their scope of application to cover wider range of slenderness, stiffening, residual stresses, shear connectors and material type of steel elements.

6. REFERENCES

- [1] Gupta V. K., Okui Y., and Nagai M., "Development of web slenderness limits for composite i-girders accounting for initial bending moment," *Doboku Gakkai Ronbunshuu A*, vol. 62, no. 4, pp. 854–864, 2006, doi: 10.2208/jsceja.62.854.
- [2] Taleb C. eddine, Ammari F., Adman R., "Analytical Study of Buckling Profile Web Stability," *Struct. Eng. Mech.*, vol. 53, no. 1, p. 147, 2015, doi: 10.12989/SEM.2014.53.1.147.
- [3] Musa I. A., "Buckling of plates including effect of shear deformations: A hyperelastic formulation," *Struct. Eng. Mech.*, vol. 57, no. 6, pp. 1107–1124, Mar. 2016, doi: 10.12989/sem.2016.57.6.1107.
- [4] Liu J., Ding F. X., Liu X. M., and Yu Z. W., "Study on flexural capacity of simply supported steel-concrete composite beam," *Steel Compos. Struct.*, vol. 21, no. 4, pp. 829–847, Jul. 2016, doi: 10.12989/scs.2016.21.4.829.
- [5] Gupta V. K., Okui Y., Inaba N., and Nagai M., "Effect of concrete crushing on flexural strength of steel-concrete composite girders," *Struct. Eng. Eng.*, vol. 24, no. 2, 2007, doi: 10.2208/jscseee.24.73s.
- [6] American Association of State Highway and Transportation Officials., *AASHTO*

- LRFD bridge design specifications, SI units: 2005 interim revisions., 3rd ed. Washington DC: American Association of State Highway and Transportation Officials, 2005.
- [7] "BS EN 1994-2:2005 - Eurocode 4. Design of composite steel and concrete structures. General rules and rules for bridges." <https://shop.bsigroup.com/ProductDetail?pid=00000000030187356> (accessed Dec. 18, 2020).
- [8] Viet D. and Okui Y., "Flexural Capacity of Composite Girders: Design Equation Accounting for Bridge High Performance Steels," 2014.
- [9] Duc D. V. and Okui Y., Flexural Capacity Accounting for SBHS500 Steel of Composite Bridge Girders, vol. 54. Springer Singapore, 2020.
- [10] Men P., Zhou X., Zhang Z, Di, J. and Qin F., "Behaviour of steel–concrete composite girders under combined negative moment and shear," J. Constr. Steel Res., vol. 179, p. 106508, Apr. 2021, doi: 10.1016/j.jcsr.2020.106508.
- [11] Bui V. T., Truong V. H., Trinh M. C., and Kim S. E., "Fully nonlinear analysis of steel-concrete composite girder with web local buckling effects," Int. J. Mech. Sci., vol. 184, p. 105729, Oct. 2020, doi: 10.1016/j.ijmecsci.2020.105729.
- [12] "Egyptian Code Of Practice For Steel Construction :(Load And Resistance Factor Design) (LRFD) 205 Ministerial Decree No 359 - 2007 /." 2012.
- [13] Abd Elrahman A. M., "A proposal of sections classification considering web slenderness of beam composite sections in the Egyptian code.," Cairo University, 2018.
- [14] Gupta V. K., Okui Y., and Nagai M., "Development of web slenderness limits for composite I-girders accounting for initial bending moment," Struct. Eng. Eng., vol. 23, no. 2, 2006, doi: 10.2208/jsce.see.23.229s.
- [15] "Steel Designers' Manual, 7th Edition | Wiley." <https://www.wiley.com/en-us/Steel+Designers%27+Manual%2C+7th+Edition-p-9781119249863> (accessed Dec. 18, 2020).
- [16] Sankar M. B. and Jacob P. A., "Comparison of Design Standards for Steel Railway Bridges," Int. J. Eng. Res. Appl., vol. 3, no. 2, pp. 1131–1138, 2013.
- [17] "Steel Designers Manual. Fifth Edition." <https://trid.trb.org/view/375463> (accessed Dec. 18, 2020).
- [18] Subramani T. and Sugathan A., "Finite Element Analysis of Thin Walled-Shell Structures by ANSYS and LS-DYNA," 2012.
- [19] ECP-201, "Egyptian Code of Practice for Calculation of Loads and Forces in Structures and Buildings.," Cairo, 2012.
- [20] Okui Y., "Design Issues for Steel-Concrete Composite Girders," Earthquake, pp. 85–93, 2011.

Copyright © Int. J. of GEOMATE. All rights reserved, including the making of copies unless permission is obtained from the copyright proprietors.
